Strong Damping of Stimulated Brillouin Scattering in Cavity-Structured Targets

K. A. Tanaka, M. Mineo, T. Boehly, T. Mochizuki, K. Nishihara, and C. Yamanaka
Institute of Laser Engineering, Osaka University, Osaka, 565 Japan
(Received 14 July 1986)

With use of a large green laser system (5 kJ, 500 psec, ten beams), scattered light from cavity and cannonball targets (1500 μm diam) is investigated. Strong suppression of stimulated Brillouin scattering is observed for the cavity target, while weak to modest suppression of stimulated Brillouin scattering is measured for the cannonball targets. The observed damping is attributed to sudden temperature rise due to collisions of two plasmas in the cavity.

PACS numbers: 42.65.Es, 52.35.Nx, 52.50.Jm, 78.35. + c

Stimulated Brillouin scattering (SBS) has been the subject of a number of experimental[1] and theoretical[2] studies. This parametric instability may potentially be a deleterious factor in laser fusion by reflecting the incoming laser light. In the past more than 50% reflection was reported due to SBS in 1-μm laser experiments[3,4] even though relatively small laser outputs were employed (<100 J). It is not well known how much laser light is scattered from a large cavity target (<2000 μm diam) by SBS when kilojoule laser energy is focused into the target. SBS could grow nonlinearly in such a plasma with a long density scale length of the target since the laser intensity can be as high as 10^{17} W/cm^2.

We observed scattered light at around the fundamental wavelength in experiments using cannonball[5] and cavity-type targets irradiated with 0.53-μm laser light. Two types of targets were used: a hollow plastic shell with two inlet holes (*A* type) and a cannonball target which has a Au outer shell with two inlet holes and a plastic-coated inner pellet (*B* and *C* types). The *B*- and *C*-type shots only differed in the irradiation intensity; the *C*-type target was irradiated at one-fourth the intensity used for the *B* type. The temporally and spectrally resolved backscattered light with a time fiducial showed a clear suppression of SBS at around the time of the incident laser peak when a plastic cavity target (*A* type) was used. SBS from Au cannonball targets (*B* type) showed a similar but less pronounced sign of the suppression, which may be attributed to the slow expansion speed of heavy Au plasmas. As for the cannonball targets, fractional backscattered energy due to SBS was 16% for the standard target (*B* type) irradiated with 4.3-kJ energy. 30% of the backscattered fraction was observed for the standard target with one-fourth the incident energy (*C* type). On the latter shot no clear saturation of SBS was observed.

Experiments were carried out by use of the Gekko XII laser system at the Institute of Laser Engineering, Osaka University. The Nd-doped glass laser system has twelve beams with final diameters of 35 cm. The second harmonic of 1-μm laser light was used and output energies with ten out of twelve beams at 0.53 μm were up to 5 kJ with a temporally Gaussian pulse of 500 psec full width at half maximum (FWHM). Cavity-type targets (*A* type) of 1500 μm diameter have two 500-μm-diam entrance holes for the incoming laser light. The shell was 30-μm-thick C_8H_8 (plastic). A bundle of five beams was focused onto the center of each entrance hole. The laser beam intensity at the first bounce of the inner wall is about 7×10^{14} W/cm^2 for 400 J per beam, while the highest intensity is at the best focus point and is about 1×10^{17} W/cm^2. The angle of incidence is 57° at the inside wall of the target.

As shown in Fig. 1, standard cannonball targets (*B* and *C* types) consisted of a 1500-μm (Au 10 μm thickness) outer shell with two 500-μm entrance holes and a 500-μm inner shell which was a glass microballoon coated with plastic (1.4 μm). The inner shell was supported by a 0.3-μm-thick plastic film. The placement accuracy of the inner shell was within 50 μm from the center of the outer shell.

Figure 2 shows a datum of the time-resolved backscattered spectrum from an *A*-type target (plastic cavity). The data are displayed as optical density contours with uniform step size. Time zero corresponds to the peak of the incident laser pulse, which has been determined with a separate time fiducial. Time proceeds from bottom to top,

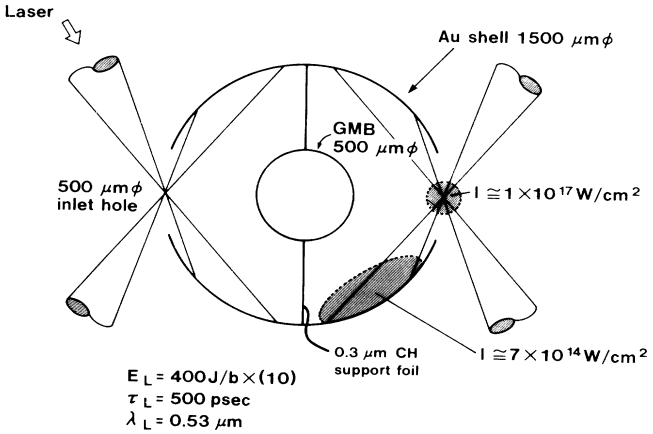

FIG. 1. Specifications of cannonball target.

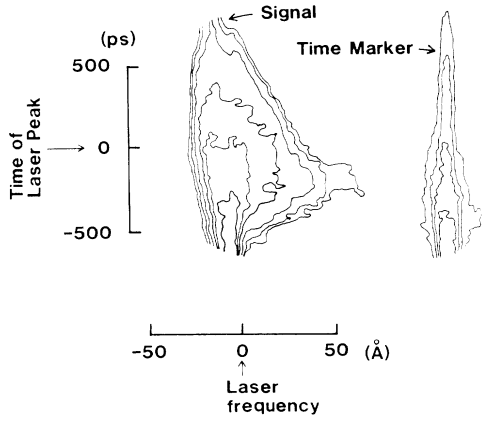

FIG. 2. Time-resolved backscattered spectrum with time marker for A-type target. The data are displayed in iso-optical-density contours. From the time marker, time of laser peak is determined in the backscattered signal.

while wavelength increases towards the right. The spectrum shows a sharp increase in the intensity much faster than the rise time of the laser pulse and a large red shift ($\Delta\lambda_{max}=30$ Å) is noted at the beginning of the pulse. These observed characteristics are consistent with SBS. From the frequency-matching condition for the instability $\Delta\lambda$ should be 5 Å or more. The backscattered light should also be strongly collimated if SBS is responsible for the reflection. Optical calorimetry was used to monitor both the backscattered (back through the lens) and sidescattered light (rest of the chamber). From the calorimetry measurements, the energy per solid angle was typically 10 times more for the backscattered light than for the sidescattered light, consistent with SBS. It should be noted that the intensity of the backscattered light and the amount of the red shift start decreasing at around the laser pulse peak.

Figures 3(a) and 3(b) are the data of the B- and C-type targets. Two inlet holes (500 μm diam) were located in the outer shell as shown in Fig. 1. The only difference of the experimental conditions between types B and C was the irradiation intensity. The intensity used for Fig. 3(a) is 7×10^{14} W/cm^2 at the first bounce of the wall (type B) while one-fourth of this intensity was used for Fig. 3(b) (type C). We note that there are several points in common between the data in Fig. 2 and Fig. 3(a). In both figures the backscattered light shows increasing red shifts in time. The saturation of the intensities and the red shifts occur before the laser pulse peak. However, the backscattered intensity of type C, Fig. 3(b), decreases much more slowly than that of type B, indicating that the damping mechanism works less effectively for the type C. This should cause a higher fraction of backscattered light for type C than for type B. The energy fractions of the backscattered light for each type are 18% for A, 16% for B, and 30% for type C. These results were somewhat

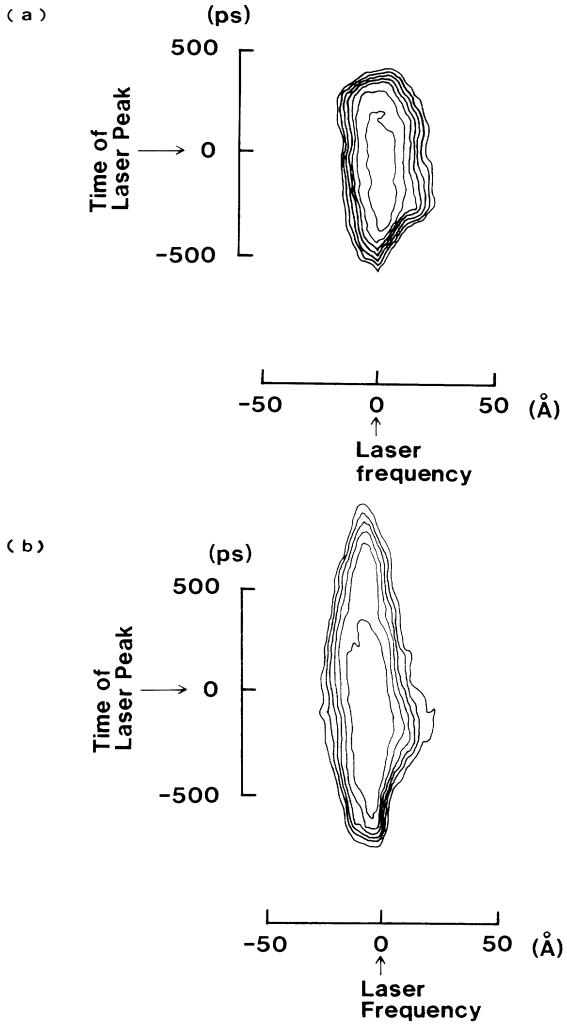

FIG. 3. (a) Time-resolved backscattering spectrum for B-type target. (b) Time-resolved backscattering spectrum for C-type target.

surprising. We expected that SBS should show a nonlinear decrease from type B to type C since the pumping intensity was reduced to a quarter of the type-B intensity for type C (i.e., 2×10^{14} W/cm^2), close to the SBS threshold intensity. The estimated threshold value for SBS is $I_{SBS}=(1-2)\times10^{14}$ W/cm^2 for plasma parameters density scale length $L_n=100-200$ μm, ratio of the electron plasma density where SBS occurs to the critical density $n_e/n_c=1/10$, and plasma electron temperature $T_e=500-1000$ eV. Although the density scale length above may be an underestimated one considering the target sizes, the intensity (I_{SBS}) should indicate a lower limit for the threshold. The red shifts from these cannonball targets (types B and C) were smaller than that from the plastic cavity target (type A). The smaller red shifts observed in Fig. 3 are consistent with the fact that the shift

$\Delta\lambda$ due to SBS[6] is proportional to the inverse square root of Am_p on the assumption that the coronal temperature (ZT_e) does not vary so much. Here Am_p is the ion mass. The collimation of the light was as strong as for the A type. We consider that the backscattered light from these Au cannonball targets is also due to SBS.

We observe that the main reflection mechanism for both low-Z cavities and high-Z cannonball targets is due to SBS. Very strong damping of the scattered light for type A, moderate damping for type B, and a low level of damping for type C are observed. The fractional backscattered light (A and B types) is typically less than 20% except for the C-type target, which shows as much as 30%. In the experiment various parameters of the cannonball target were tested to observe any difference in the backscattered energy, but no distinctive deviation was observed from the results for type B. The changed parameters include the target size (<2000 μm), the inlet hole size (750 μm), and the smaller aspect ratio ($r_{\text{asp}}=2$). Here the aspect ratio is defined as the ratio of the outer-shell diameter to the inner-shell diameter. Very strong damping of the scattered light for type A, moderate damping for type B, and a low level of damping for type C are observed.

There are several mechanisms responsible for the damping of SBS, such as Landau damping of ion waves,[6] ion trapping,[7] and nonlinear frequency shift, etc. Ion heating time would be too long in these mechanisms to be observed as strong damping within a laser pulse, since the partitioning from the laser energy to the ion energy is of the order of ω_{ia}/ω_L. ω_{ia} and ω_L are the ion acoustic and laser frequencies. For example, about 2 nsec would be needed to heat ions through ion Landau damping[6] with the parameters used in this experiment. Since the strong damping which we have observed has never been reported, we conclude that the damping could result from an abrupt change in the plasma condition due to the special structure of these targets.

In the A-type target, laser light not absorbed at the first or subsequent bounces will ablate the edge of the entrance hole on the other side. The plasmas from the edges collide at the center of the holes, and then the ion temperature increases rapidly as the kinetic energy is converted into the thermal energy. For the cannonball targets the plasmas collide also within the cavity between the inner and outer shells. These hydrodynamic motions are simulated by the 1D hydrodynamic code HISHO in which laser ray trajectories are treated in 3D.[8] Figure 4 shows the ratios of ion to electron temperatures near the one-tenth–critical electron density with average ionization state Z. In HISHO laser absorption is treated, with inverse bremsstrahlung absorption along the laser ray trajectory and resonance absorption at the turning point. The value of $k_0L=10$ was assumed for resonance absorption, where k_0 and L are the wave number of the laser light and the scale length of the density gradient at critical density. The calculation of absorption is stopped when the cavity

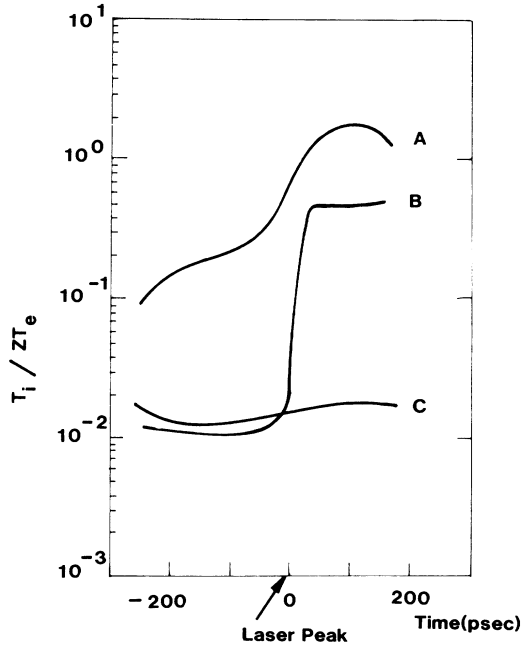

FIG. 4. Simulation results of ion temperature histories for A-, B-, and C-type targets near one-tenth critical density. The labeling of the curves corresponds to the type of targets.

between the shells is filled by the expanding plasmas from the shells. Figure 4 indicates that for both A (curve A) and B (curve B) types the ratios of ion to electron temperatures increase suddenly at around the peak of the pulse. The increase for the A type is much higher than that for the B type because the A type has only low-Z plasmas (CH) while both low and high Z (Au) are involved for the B type. Though the timing of the ion temperature rises in Fig. 4 for the A and B types seems to be consistent with the data shown in Fig. 2 and Fig. 3(a), this should be fortuitous. Since the timing of the plasma collision depends on the local energy deposition by laser and the structure of the plasma formation, these simulation results should be used as a guide line to understand the complicated behavior of the nonlinear processes. For the C type (curve C in Fig. 4) the temperature ratio is approximately constant. Since the irradiation intensity of the C type is one-fourth the intensity for the B type, causing a much slower plasma expansion, the plasmas from outer and inner shells therefore do not collide during the laser pulse. The difference in the temperature ratio for the B and C type is clear; the ratio increases from 10^{-2} to 5×10^{-1} for the B type and increases from 1.5×10^{-2} only to 2×10^{-2} for the C type. Landau damping should become effective when T_i/ZT_e exceeds the value of 0.1. Thus, strong Landau damping may not be expected for the C type because of the low value of the temperature ratio. The damping, in turn, should be most effective for the A, then next for the B type after the ion temperature rises. These calculation results are qualitatively in good

agreement with the observed timing and the level of SBS suppression.

The backscattered light from the low-Z cavity and high-Z cannonball targets is spectrally and temporally resolved for the first time. The results indicate that the main reflection mechanism is due to SBS. Less than 20% of the backscattered energy is observed for most of the target types except 30% for the C type. Strong to moderate damping is observed for the A (low-Z cavity) and B (high-Z cannonball) targets. Simulation results for these target parameters indicate that when the plasmas from the inner and outer shells collide, then the ratio T_i/ZT_e increases to a level at which strong Landau damping could occur. We conclude that the observed damping is due to the result of the plasma collisions in these specially structured targets.

We would like to thank Professor K. Mima for suggesting the idea of ion heating due to the plasma collisions. We are indebted to Dr. S. Nakai, Dr. M. Nakatsuka, Dr. M. Yamanaka, Dr. S. Ido, Dr. H. Azechi, Dr. N. Miyanaga, Dr. H. Nishimura, Dr. T. Norimatsu, Dr. T. Jitsuno, and Dr. M. Murakami, and the T-, M-, and GOD-groups.

[1]L. M. Goldman, J. Soures, and M. L. Lubin, Phys. Rev. Lett. **31**, 1184 (1973); J. J. Turechek and F. F. Chen, Phys. Rev. Lett. **36**, 720 (1976); B. H. Ripin, F. C. Young, J. A. Stamper, C. M. Armstrong, and R. Decoste, Phys. Rev. Lett. **39**, 611 (1977); L. M. Gorbunov, Y. S. Kas'yanov, V. V. Korobkin, A. N. Polyanichev, and A. P. Shevel'ko, Pis'ma Zh. Eksp. Teor. Fiz. **27**, 242 (1978) [JETP Lett. **27**, 227 (1978)]; M. J. Herbst, C. E. Clayton, and F. F. Chen, J. Appl. Phys. **51**, 4080 (1980); R. E. Turner and L. M. Goldman, Phys. Rev. Lett. **44**, 400 (1980); J. Benard and J. Meyer, Phys. Rev. Lett. **55**, 79 (1985); K. A. Tanaka, B. Boswell, R. S. Craxton, L. M. Goldman, F. Guglielmi, W. Seka, R. W. Short, and J. M. Soures, Phys. Fluids **28**, 2910 (1985).

[2]C. L. Tang, J. Appl. Phys. **37**, 2945 (1966); D. W. Forslund, J. M. Kindel, and E. L. Lindman, Phys. Fluids **18**, 1002 (1975).

[3]B. H. Ripin, Appl. Phys. Lett. **30**, 134 (1977).

[4]K. Tanaka and L. M. Goldman, Phys. Rev. Lett. **45**, 1558 (1980).

[5]H. Azechi, N. Miyanaga, S. Sakabe, T. Yamanaka, and C. Yamanaka, Jpn. J. Appl. Phys. **20**, L477 (1981); T. Boehly, K. A. Tanaka, T. Mochizuki, K. Nishihara, Y. Sakawa, M. Murakami, K. Sakurai, and C. Yamanaka, Opt. Commun. (to be published).

[6]W. L. Kruer, Phys. Fluids **23**, 1273 (1980).

[7]C. E. Clayton, C. Joshi, and F. F. Chen, Phys. Rev. Lett. **51**, 1656 (1983).

[8]M. Murakami and K. Nishihara, Institute for Laser Engineering, Osaka University, Quarterly Progress Report No. ILE-QPR-83-6, 1983 (unpublished), p. 34.